Endogenous Diterpenes Derived from *ent*-Kaurene, a Common Gibberellin Precursor, Regulate Protonema Differentiation of the Moss *Physcomitrella patens*[1][W][OA]

Ken-ichiro Hayashi*, Keisuke Horie, Yuji Hiwatashi, Hiroshi Kawaide, Shinjiro Yamaguchi, Atsushi Hanada, Tamotsu Nakashima, Masatoshi Nakajima, Lewis N. Mander, Hisakazu Yamane, Mitsuyasu Hasebe, and Hiroshi Nozaki

Department of Biochemistry, Okayama University of Science, Okayama 700–0005, Japan (K.-i.H., K.H., T.N., H.N.); National Institute for Basic Biology, Okazaki 444–8585, Japan (Y.H., M.H.); School of Life Science, Graduate University for Advanced Studies, Okazaki 444–8585, Japan (Y.H., M.H.); Institute of Agriculture, Tokyo University of Agriculture and Technology, Fuchu, Tokyo 183–8509, Japan (H.K.); RIKEN Plant Science Center, Tsurumi, Yokohama 230–0045, Japan (S.Y., A.H.); Department of Applied Biological Chemistry (M.N.) and Biotechnology Research Center (H.Y.), University of Tokyo, Tokyo 113–8657, Japan; Research School of Chemistry, Australian National University, Canberra, Australian Capital Territory 0200, Australia (L.N.M.); and ERATO, Japan Science and Technology Agency, Okazaki 444–8585, Japan (M.H.)

Gibberellins (GAs) are a group of diterpene-type plant hormones biosynthesized from *ent*-kaurene via *ent*-kaurenoic acid. GAs are ubiquitously present in seed plants. The GA signal is perceived and transduced by the GID1 GA receptor/DELLA repressor pathway. The lycopod *Selaginella moellendorffii* biosynthesizes GA and has functional GID1-DELLA signaling components. In contrast, no GAs or functionally orthologous GID1-DELLA components have been found in the moss *Physcomitrella patens*. However, *P. patens* produces *ent*-kaurene, a common precursor for GAs, and possesses a functional *ent*-kaurene synthase, PpCPS/KS. To assess the biological role of *ent*-kaurene in *P. patens*, we generated a PpCPS/KS disruption mutant that does not accumulate *ent*-kaurene. Phenotypic analysis demonstrates that the mutant has a defect in the protonemal differentiation of the chloronemata to caulonemata. Gas chromatography-mass spectrometry analysis shows that *P. patens* produces *ent*-kaurenoic acid, an *ent*-kaurene metabolite in the GA biosynthesis pathway. The phenotypic defect of the disruptant was recovered by the application of *ent*-kaurene or *ent*-kaurenoic acid, suggesting that *ent*-kaurenoic acid, or a downstream metabolite, is involved in protonemal differentiation. Treatment with uniconazole, an inhibitor of *ent*-kaurene oxidase in GA biosynthesis, mimics the protonemal phenotypes of the PpCPS/KS mutant, which were also restored by *ent*-kaurenoic acid treatment. Interestingly, the GA_9 methyl ester, a fern antheridiogen, rescued the protonemal defect of the disruption mutant, while GA_3 and GA_4, both of which are active GAs in angiosperms, did not. Our results suggest that the moss *P. patens* utilizes a diterpene metabolite from *ent*-kaurene as an endogenous developmental regulator and provide insights into the evolution of GA functions in land plants.

GAs are a large family of tetracyclic diterpenoids, and bioactive GAs play crucial roles in aspects of plant growth and development, including seed germination, stem elongation, leaf expansion, trichome development, and flower and fruit development (Olszewski et al., 2002). GAs are biosynthesized from *ent*-kaurene, the key intermediate of the GA biosynthetic pathway (Olszewski et al., 2002; Yamaguchi, 2008; Fig. 1). *ent*-Kaurene is synthesized via sequential cyclization steps of geranylgeranyl diphosphate (GGDP) by *ent*-copalyl diphosphate synthase (CPS; Sun and Kamiya, 1994) and *ent*-kaurene synthase (KS; Yamaguchi et al., 1996, 1998). The bioactive GAs (GA_1 and GA_4) are synthesized through a series of oxidation reactions of *ent*-kaurene by two types of oxidases. Both *ent*-kaurene oxidase and *ent*-kaurenoic acid oxidase are cytochrome P450 monooxygenases that successively convert *ent*-kaurene to GA_{12}. GA_{12} is further converted to bioactive GAs by two 2-oxoglutarate-dependent dioxygenases, GA 20-oxidase and GA 3-oxidase (Phillips et al., 1995; Olszewski et al., 2002; Yamaguchi, 2008; Fig. 1). GA 2-oxidase is another member of the

[1] This work was supported by a Japan Society for the Promotion of Science Grant-in Aid for Scientific Research (no. 20510210) to H.N., by the Japan Society for the Promotion of Science and the Ministry of Education, Culture, Sports, Science and Technology of Japan to M.H., and by a matching fund subsidy for private universities from the Ministry of Education, Culture, Sports, Science and Technology of Japan to K.-i.H.

* Corresponding author; e-mail hayashi@dbc.ous.ac.jp.

The author responsible for distribution of materials integral to the findings presented in this article in accordance with the policy described in the Instructions for Authors (www.plantphysiol.org) is: Ken-ichiro Hayashi (hayashi@dbc.ous.ac.jp).

[W] The online version of this article contains Web-only data.

[OA] Open Access articles can be viewed online without a subscription.

www.plantphysiol.org/cgi/doi/10.1104/pp.110.157909

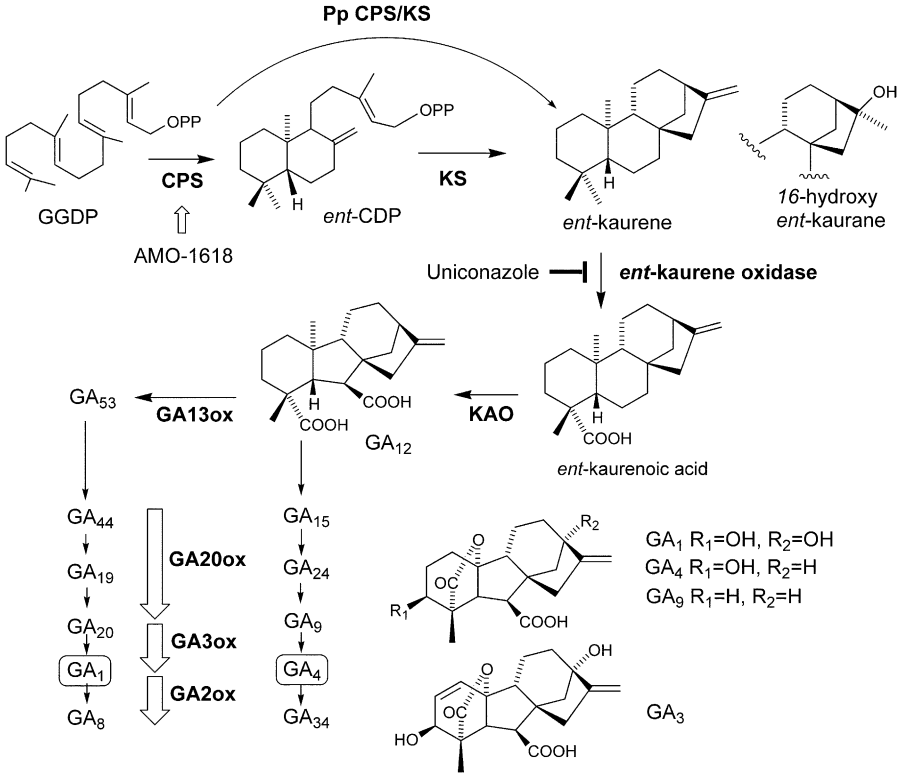

Figure 1. The biosynthetic pathway of GA. The enzyme names are shown in boldface below or to the right of each arrow. AMO-1618 is an angiosperm inhibitor of CPS. Uniconazole, a GA biosynthesis inhibitor, blocks *ent*-kaurene oxidase activity. GA_1 and GA_4 are the bioactive GAs, and GA_8 and GA_{34} are their inactive catabolites, respectively. KAO, *ent*-Kaurenoic acid oxidase.

2-oxoglutarate-dependent dioxygenase family and is responsible for GA inactivation (Fig. 1). The active GAs can bind to the soluble GA receptor, GID1, and promote the interaction of GID1 with DELLA repressors, which are negative regulators of GA signaling (Ueguchi-Tanaka et al., 2005; Nakajima et al., 2006). This GA-promoted GID1-DELLA interaction triggers the degradation of DELLA repressors via the $SCF^{GID2/SLY1}$ proteasome pathway and consequently activates GA signaling (Ueguchi-Tanaka et al., 2007).

In nonseed land vascular plants, auxin, cytokinin, and abscisic acid function as regulators of plant growth and development (Chopra and Kumra, 1988; Raghavan, 1989). Various physiological responses to these phytohormones are investigated in nonseed land plants, especially in the model moss *Physcomitrella patens* (Cove et al., 2006). Auxin and cytokinin function in developmental phase changes of chloronemata, caulonemata, and gametophores as well as in cellular growth regulation in *P. patens* (Imaizumi et al., 2002; Sakakibara et al., 2003; Decker et al., 2006). Abscisic acid mediates the establishment of tolerance to dehydration, cold temperature, and osmotic stresses in *P. patens* as in angiosperms (Decker et al., 2006; Cho et al., 2009; Khandelwal et al., 2010). In contrast to these hormones, there are only a few studies on the physiological activity of GA in mosses (Von Maltzahn and Macquarrie, 1958; Chopra and Mehta, 1987; Vandenbussche et al., 2007), and the GA function and signaling pathways are still unclear.

Recent progress in plant molecular biology and chemical analysis of GA revealed the biosynthesis, perception, and signaling of GA in *P. patens* and the lycopod *Selaginella moellendorffii* (Hirano et al., 2007; Vandenbussche et al., 2007; Yasumura et al., 2007). Genome sequence for these organisms has enabled the identification of genes orthologous to flowering plant genes encoding GA biosynthetic enzymes and GA signaling components involved in the GID1-DELLA pathway (Hirano et al., 2007; Vandenbussche et al., 2007). Recently, two reports demonstrated that GID1-DELLA-mediated signaling is functionally conserved in the fern *Selaginella* and in angiosperms (Hirano et al., 2007; Yasumura et al., 2007). GA-dependent protein-protein interactions were observed between SmGID1 and SmDELLA proteins, the *S. moellendorffii* proteins orthologous to the rice (*Oryza sativa*) GID1 and DELLA proteins, respectively. The introduction of either the *SmGID1a* or *SmGID1b* gene rescued the rice *Osgid1-3* mutant, and the overproduction of *SmDELLA1* suppressed GA action in the wild-type background. These reports indicate that the GID1 and DELLA proteins function similarly in *S. moellendorffii* and in angiosperms. Additionally, *S. moellendorffii* has functional GA biosynthetic enzymes similar to the angiosperm GA 20- and GA 3-oxidases and endogenous active GA_4 detected by liquid chromatography-tandem mass spectrometry (LC-MS/MS) analysis. However, endogenous GAs were not detected in *P. patens* by LC-MS/MS analysis, and the putative

P. patens GA oxidases did not show any enzymatic activity on the known substrate for the orthologous angiosperm GA oxidases (Hirano et al., 2007). Furthermore, the PpGID1-like and PpDELLA-like proteins did not interact in the presence of active GA in yeast cells, and the PpDELLA-like protein did not complement the rice DELLA function. These findings suggest that GID1-DELLA-mediated GA signaling evolved in the vascular plant lineage after bryophyte divergence (Hirano et al., 2008).

GA_1 and GA_4 are recognized as major biologically active GAs in angiosperms. *S. moellendorffii* biosynthesizes GA_4 as an active GA. Additionally, the Schizaeaceae family of ferns utilize GA methyl esters (methyl esters of GA_9, GA_{20}, and GA_{73}) as regulators of antheridium development, whereas these GA methyl esters are inactive in angiosperms (Yamauchi et al., 1996, 1997; Kurumatani et al., 2001). The biologically active GAs present in angiosperms were not detected in *P. patens* (Hirano et al., 2007). Although diverse GA metabolites have been found in plants and fungi, all the GA metabolites are thought to be derived from *ent*-kaurene, a common intermediate in early GA biosynthetic steps in both land plants and fungi (Kawaide, 2006). In angiosperms, two separate enzymes (CPS and KS) are involved in *ent*-kaurene synthesis from GGDP via *ent*-copalyl diphosphate as a reaction intermediate (Fig. 1). We have reported that PpCPS/KS, catalyzing the direct cyclization of GGDP to *ent*-kaurene, was a bifunctional diterpene cyclase with both CPS and KS activities in a single polypeptide (Hayashi et al., 2006). This type of bifunctional *ent*-kaurene synthase was also found in GA-producing fungi but was not identified in angiosperms (Kawaide et al., 1997; Toyomasu et al., 2000). The *P. patens* genome contains a single CPS/KS homolog, and no diterpene cyclase gene was found on the basis of sequence similarity in this organism. Anterola et al. (2009) reported that AMO-1618, an inhibitor of CPS, suppressed spore germination in *P. patens*; the suppression was recovered by exogenous *ent*-kaurene application. These results led the authors to hypothesize a role for *ent*-kaurene in regulating spore germination (Anterola et al., 2009). However, the hypothesis should be examined because the AMO-1618 inhibitory effect was not fully recovered by *ent*-kaurene application, probably because of the unspecific inhibitory effect of AMO-1618 on spore germination (Anterola et al., 2009).

To assess the biological role of *ent*-kaurene and its metabolites in *P. patens*, we performed an insertional knockout of the *ent*-kaurene synthase gene, *CPS/KS*, in *P. patens*; the loss of *ent*-kaurene production was confirmed by gas chromatography-mass spectrometry (GC-MS) analysis. We also determined the abundance of all possible GAs and their precursors in *P. patens* by LC-MS/MS analysis. The *PpCPS/KS* disruption mutant (Ppcps/ks KO) lines have a defect in protonemal development. The differentiation of chloronemata to caulonemata was suppressed in the Ppcps/ks KO mutants, and the defect was recovered by the exogenous application of *ent*-kaurene or *ent*-kaurenoic acid. Furthermore, the GA_9 methyl ester, an antheridiogen of schizaeaceous ferns, rescued the protonemal defect of the mutants, but GA_3 and GA_4, the representative active GAs for angiosperm, did not. Our results demonstrate that *P. patens* utilizes GA-type diterpenes synthesized from *ent*-kaurene as an endogenous growth regulator in protonemal development.

RESULTS

GA-Related Metabolites in *P. patens*

Hirano et al. (2007) measured GAs, including GA_{24}, GA_9, GA_4, GA_{19}, GA_{20}, and GA_1, in the late stage of the pathway (Fig. 1) in *P. patens* by LC-MS/MS analysis and reported that none of these were detectable. To examine whether any earlier metabolites in the GA pathway occur in *P. patens*, we analyzed all measurable GAs in our system (including those analyzed by Hirano et al. [2007]) and their precursor *ent*-kaurenoic acid in *P. patens* by LC-MS/MS or GC-MS using deuterium-labeled compounds as internal standards (Table I; Supplemental Fig. S1). *ent*-Kaurenoic acid was identified by full-scan GC-MS (Supplemental Fig. S2),

Table I. *Endogenous levels of GAs and ent-kaurenoic acid in P. patens*

GA Metabolite	Level[a]	GA Metabolite	Level[a]
	ng g^{-1} fresh wt		*ng g^{-1} fresh wt*
GA_1	n.d.[b]	GA_{29}	n.d.
GA_4	n.d.	GA_{34}	n.d.
GA_8	n.d.	GA_{44}	n.d.
GA_9	n.d.	GA_{51}	n.d.
GA_{12}	n.d.	GA_{53}	n.d.
GA_{15}	n.d.	*ent*-Kaurenoic acid (1 week old)[c]	87.5
GA_{19}	n.d.	*ent*-Kaurenoic acid (2 weeks old)	239.9
GA_{20}	n.d.	*ent*-Kaurenoic acid (3 weeks old)	137.2
GA_{24}	n.d.		

[a]Protonemata in white light for 10 d. [b]n.d., Not detected. [c]Length of the cultivation of protonemal colonies.

while none of the measured GAs were detected in our *P. patens* protonemata (Supplemental Fig. S1). Previous studies have shown that the vegetative tissues of Arabidopsis and the fern *S. moellendorffii* contain approximately 1 ng g^{-1} dry weight (Hu et al., 2008) and 1 ng g^{-1} fresh weight GA_4, respectively (Hirano et al., 2007). From LC-MS/MS measurement, GA_4 is presumably not present in *P. patens*, but if it is the amount must be less than 1.5 pg g^{-1} fresh weight (Supplemental Fig. S1). These results indicate that all GAs in the major angiosperm pathway accumulate at much lower levels in *P. patens* than in angiosperms. In contrast, *P. patens* produces a considerably larger amount of *ent*-kaurenoic acid (88–200 ng g^{-1} fresh weight), suggesting the occurrence of the angiosperm GA pathway up to the steps catalyzed by *ent*-kaurene oxidase in *P. patens* (Table I; Supplemental Fig. S2).

Targeted Knockout of *CPS/KS* Gene in *P. patens*

To block *ent*-kaurene biosynthesis in *P. patens*, and to investigate the function of *ent*-kaurene, the *PpCPS/KS* gene was disrupted by replacing a genomic region containing the seventh exon and a part of the eighth exon with a resistance marker cassette by homologous recombination (Fig. 2A). The disruption of the *PpCPS/KS* gene was confirmed by Southern-blot analysis (Fig. 2B). The loss of *ent*-kaurene production was confirmed by GC-MS analysis (Fig. 2C; Supplemental Fig. S3). Three knockout lines inserted with a hygromycin

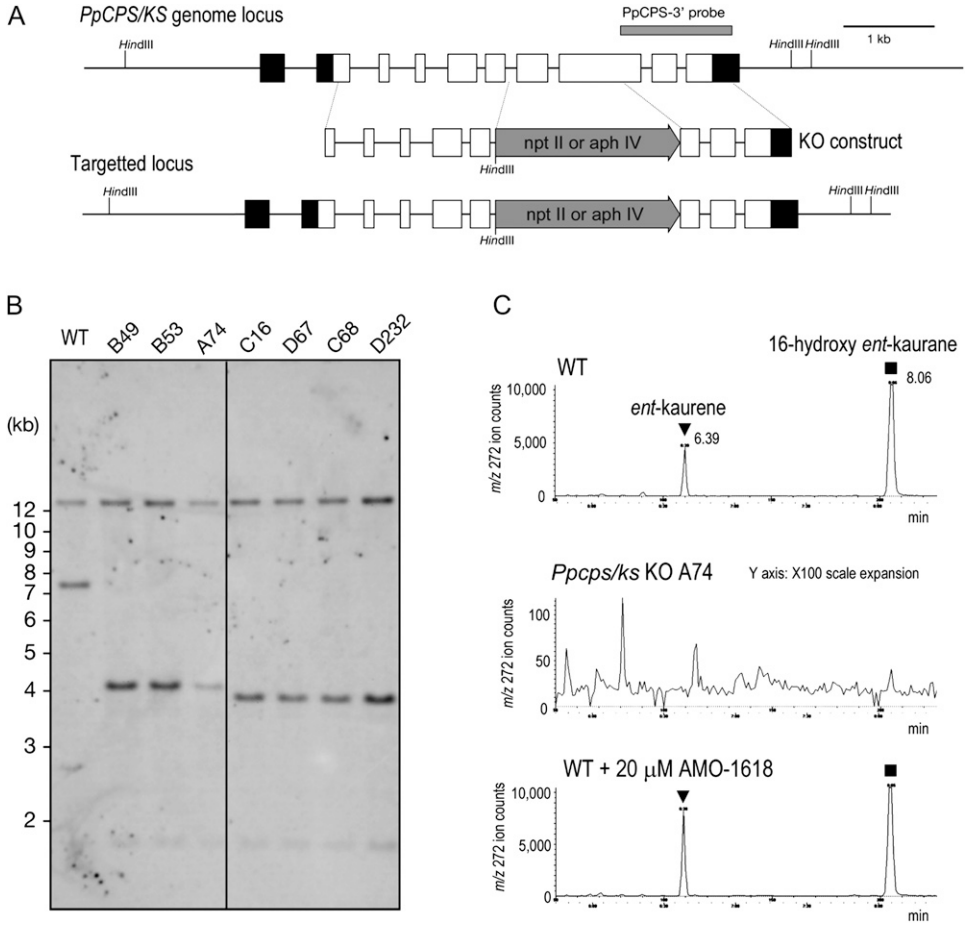

Figure 2. Disruption of *ent*-kaurene biosynthesis in *P. patens* by *CPS/KS* gene targeting. A, Genomic structures of *CPS/KS* in the wild-type and targeted Ppcps/ks KO lines. The *Hin*dIII recognition sites are indicated. Boxes and lines between the boxes indicate exons and introns, respectively. The gray arrows show the neomycin phosphotransferase II expression cassette (npt II) or the hygromycin phosphotransferase expression cassette (aph IV). The gray bar shows the position of a probe used in B. B, Southern analysis of *CPS/KS* in the wild-type and Ppcps/ks KO lines. Genomic DNA was digested with *Hin*dIII and hybridized with the probe in A. The aph IV expression cassette was inserted in the B49, B53, and A74 lines, and the npt II expression cassette was inserted in the C16, D67, C68, and D232 lines. C, GC-MS analysis of the wild type and the Ppcps/ks KO A74 line. Shown are selected ion (mass-to-charge ratio [*m/z*] 272) MS chromatograms of protonemal extracts of the wild type (top panel), Ppcps/ks KO A74 (middle panel), and the wild type treated with 20 μM AMO-1618 for 10 d of cultivation (bottom panel). The triangles and squares indicate the peaks of *ent*-kaurene and 16-hydroxy *ent*-kaurane, respectively. These kaurenes are identified by direct comparison with authentic samples. WT, Wild type.

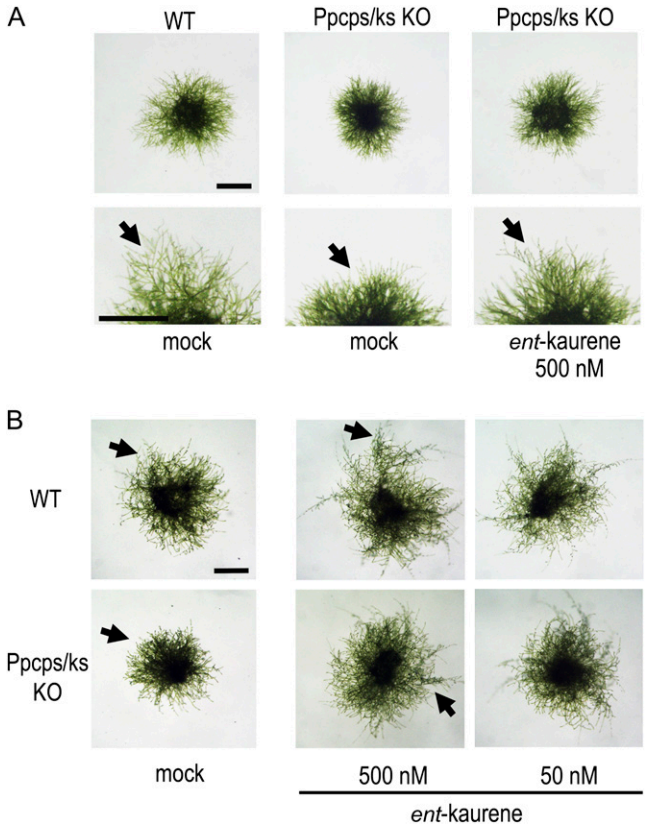

Figure 3. Ppcps/ks KO disruption mutant lines formed aberrant colonies, and exogenous *ent*-kaurene application rescued the defect. Protonemata of the wild type (WT) and the Ppcps/ks KO A74 disruptant *P. patens* were grown in the same petri dish with or without *ent*-kaurene under white light (A) or red light (B) for 6 d after inoculation on the BCD-ATG medium. Arrows indicate representative protruding caulonemata. Bars = 2 mm.

phosphotransferase expression cassette (lines A74 and B49) and a neomycin phosphotransferase II expression cassette (line C16) were used for further investigation.

The PpCPS/KS enzyme produces both *ent*-kaurene and 16-hydroxy *ent*-kaurane, a quenched product of *ent*-kaurene carbocation by water (Hayashi et al., 2006). In GC-MS analysis, both kaurenes were detected in protonemata of the wild type but not in those of the mutant lines (Fig. 2C; Supplemental Fig. S3). This result indicates that *PpCPS/KS* is entirely responsible for *ent*-kaurene production in *P. patens* protonemata.

Protonema Phenotypes of Ppcps/ks KO Lines

P. patens forms two types of protonemata, namely chloronemata and caulonemata (Cove et al., 2006). Chloronemal cells have disc-shaped chloroplasts and perpendicular septa separating the individual cells in the filaments. Chloronemal apical cells differentiate into caulonemal apical cells to form caulonemal cells, which have spindle-shaped chloroplasts and oblique septa. The rate of cell division and the speed of apical growth are faster in caulonemal apical cells than in chloronemal apical cells. A round-shaped colony mostly composed of chloronemata is formed several days after inoculation. Once differentiation from chloronemata to caulonemata starts, caulonemal filaments protrude from a colony (Fig. 3A, arrows). Differentiated chloronemata and caulonemata are reprogrammed to form stem cells called side branch initial cells. A side branch initial cell becomes a chloronemal apical cell or a gametophore apical cell.

To examine the effects of *ent*-kaurene deficiency on the moss, the morphology of protonemal colonies was observed 6 d after inoculation. Ppcps/ks KO lines formed colonies with fewer caulonemal protrusions than wild-type lines when grown under white light (Fig. 3A). To compare wild-type and Ppcps/ks KO lines under the inductive conditions for caulonemata, the lines were cultivated under red light (Imaizumi et al., 2002). Under red light, the number of protruding caulonemal filaments was decreased conspicuously in the mutant lines (Fig. 3B). As well as the enhancement of the differentiation from caulonemata to chloronemata, we suspected that the decrease in the number of side branches may induce the protrusions from colonies. However, the number of side branches in 10

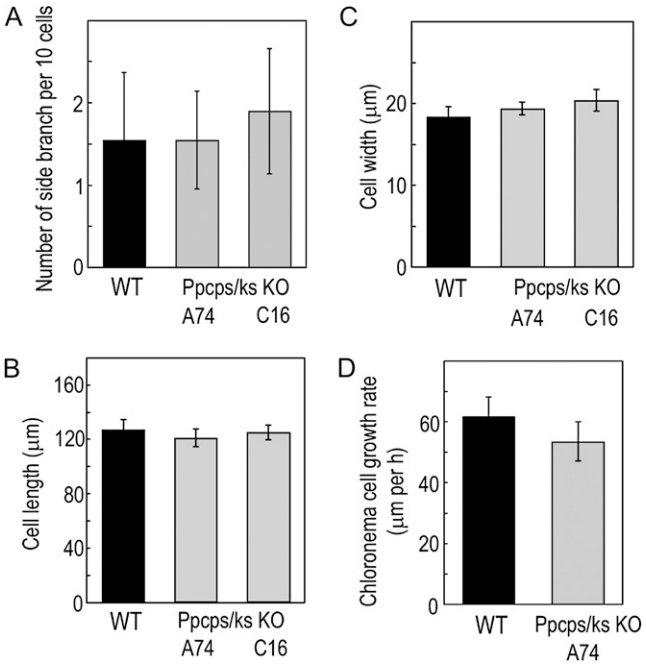

Figure 4. The number of side branches, cell size, and growth rate of protonemata in the wild-type (WT) and Ppcps/ks KO disruption lines. Chloronemata of the wild-type and Ppcps/ks KO A74 and C16 lines were grown under white light. A, Number of protonema side branches in wild-type and knockout plants. The branching among 10 cells from the apical cell was counted. B and C, The cell length and width of chloronemal cells in the wild-type and Ppcps/ks KO A74 and C16 lines. D, The cell growth rate of chloronemal cells in wild-type and knockout plants was measured. All values are averages of more than 20 chloronemal cells. Error bars represent SD.

chloronemal cells was not changed between wild-type and mutant lines (Fig. 4A). These observations indicate that the differentiation from chloronemata to caulonemata is suppressed in the mutants.

In angiosperms, the principal function of GAs in growth is the regulation of cell elongation. In *P. patens*, protonemal cells employ apical growth, and the cell size of protonemata is determined by the rate of apical growth and subsequent cellular elongation. To determine the effect of the *CPS/KS* disruption on protonemal cell growth, we examined the cell size of protonema cells. However, the average size and growth rate of protonemal cells of the mutant lines were not distinguished from those in the wild type (Fig. 4, B–D).

To test whether exogenous *ent*-kaurene rescues the mutant phenotype, protonemata were inoculated on medium containing *ent*-kaurene and cultivated for 6 d under both white and red light (Fig. 3). Exogenously applied *ent*-kaurene rescued the differentiation of chloronemata to caulonemata in the mutant line. Additionally, under red light, *ent*-kaurene application not only rescued the phenotype of the mutant lines but also enhanced caulonemata formation in the wild type on medium containing 500 nM *ent*-kaurene. These results suggest that the *ent*-kaurene produced by *PpCPS/KS* functions to enhance the differentiation from chloronemata to caulonemata.

P. patens has an orthologous gene to the angiosperm *ent*-kaurene oxidase (XP_001782544; CYP701B1) and produces *ent*-kaurenoic acid as the metabolite in protonemata (Table I). Under red light, *ent*-kaurenoic acid treatment rescued the mutant phenotype and further induced the caulonemal cell formation in the wild type (Fig. 5; Supplemental Fig. S4). Uniconazole is a GA biosynthesis inhibitor (Swain et al., 2005) that blocks the conversion of *ent*-kaurene to *ent*-kaurenoic acid by *ent*-kaurene oxidase (Fig. 1). To investigate the effect of the inhibitor, protonemata were inoculated on medium supplemented with uniconazole and cultivated under red light (Fig. 5). Uniconazole treatment at 2 μM reduced the caulonemal cell formation of the wild type to a similar extent as that of the mutant line, while uniconazole did not affect the protonemata differentiation in mutant lines (Fig. 5). The reduction of caulonemata formation in both wild-type and mutant lines was restored by the application of *ent*-kaurenoic acid. Uniconazole at a concentration of 5 μM inhibited the growth of chloronemata in both wild-type and mutant colonies to the same extent. The growth inhibition phenotype was not recovered by the application of *ent*-kaurenoic acid, suggesting the inhibition of P-450 oxidases other than *ent*-kaurene oxidase by uniconazole.

These results indicate that diterpene metabolites from *ent*-kaurene via *ent*-kaurenoic acid are involved in the developmental process of transition from chloronemata to caulonemata.

Gametophores, Sporophytes, and Spore Germination Rates in CPS/KS Disruption Mutants Were Not Different from Those in the Wild Type

In seed plants, one of the prominent effects of GAs is shoot elongation (Olszewski et al., 2002). To investigate whether diterpene metabolites from *ent*-kaurene via *ent*-kaurenoic acid have similar physiological roles to seed plant GAs, we examined the effect of PpCPS/KS disruption in the growth of gametophores, which

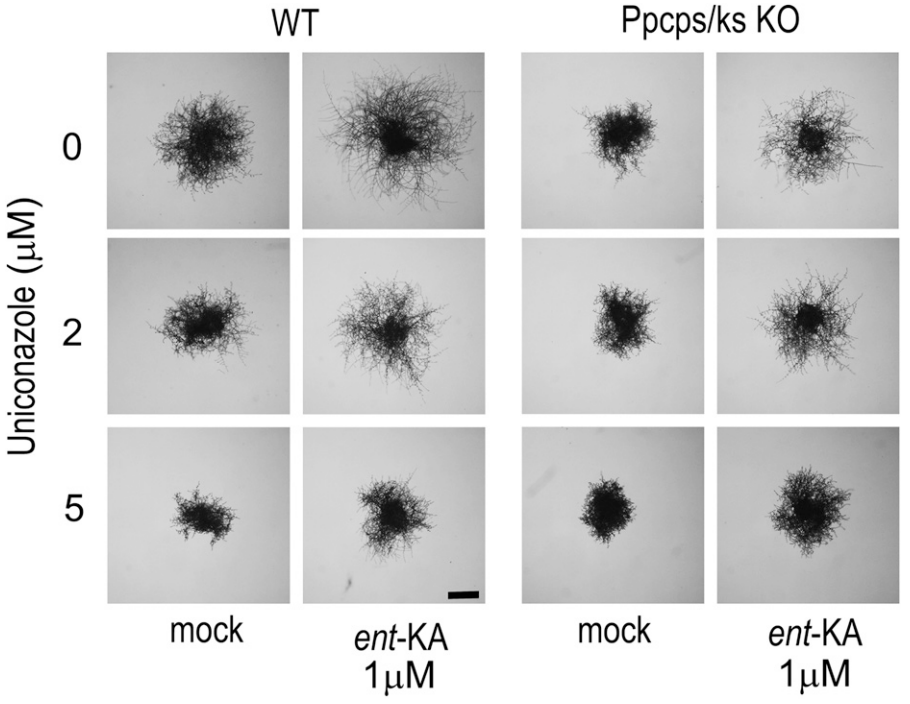

Figure 5. The effects of *ent*-kaurenoic acid and uniconazole on the differentiation of chloronemata to caulonemata in wild-type *P. patens* and the Ppcps/ks KO A74 line. Chloronemal colonies of the wild type (WT) and Ppcps/ks KO A74 were cultured in the presence or absence of *ent*-kaurenoic acid (*ent*-KA) and uniconazole under red light for 9 d on BCD-ATG medium. Representative images of protonemal colonies after cultivation are shown. Bar = 1 mm.

are analogous leafy bodies of mosses to seed plant shoots. However, the length of the stem was not different between wild-type and disruption lines (Fig. 6, A and B).

AMO-1618 was reported to inhibit the PpCPS/KS enzyme and suppress spore germination in *P. patens* (Anterola et al., 2009). This suggests that *ent*-kaurene metabolites are necessary for spore germination. To obtain spores, gametophores were cultivated under gametangial inductive conditions and sporophytes were formed. The percentage of gametophores with a sporophyte in the mutant lines was not different from that of the wild type, indicating that functional gametangia are formed for fertilization (Fig. 6C). The mutant lines formed sporophytes with spores, as did the wild-type plants (Fig. 6D). Unexpectedly, spores of the mutant lines germinated at the same rates as those of the wild type (Fig. 6E), indicating that the *ent*-kaurene metabolites are not necessary for spore germination. Furthermore, we investigated the effect of AMO-1618 on the differentiation to caulonemata and found that AMO-1618 did not cause any defects (Supplemental Fig. S5). GC-MS analysis indicated that the same levels of *ent*-kaurene were detected in protonemata grown with or without 20 μM AMO-1618 for 10 d (Fig. 2C). Taken together, these results indicate that AMO-1618 inhibits spore germination via a pathway different from that leading to *ent*-kaurene production.

GA-Type Diterpene Produced from *ent*-Kaurene Is Involved in Protonemal Development

GA_3 and GA_4 are active GAs in angiosperms, but these compounds did not show any profound effects on *P. patens* at physiological concentration (Vandenbussche et al., 2007; Yasumura et al., 2007). GA_9 methyl ester and GA_{73} methyl ester have been identified as antheridiogens that induce antheridium formation in the schizaeaceous fern *Lygodium*, but they are inactive GAs in angiosperms (Yamauchi et al., 1996; Kurumatani et al., 2001). Antheridic acid is an antheridiogen in several species of the *Anemia* genus, and GA_{103} is thought to be a precursor of antheridic acid (Yamane et al., 1988). We examined the effect of these GAs and GA-related compounds on the differentiation of chloronemata to caulonemata in *P. patens*.

GA_3 and GA_4 showed no effects on the differentiation to caulonemata in the wild type or the Ppcps/ks KO mutant under red light (Fig. 7; Supplemental Fig. S6). Additionally, GA_3 and GA_4 did not rescue the inhibition of caulonemata formation by uniconazole (Supplemental Fig. S6). Interestingly, the GA_9 methyl ester restored the differentiation to caulonemata in both the Ppcps/ks KO mutant and the uniconazole-treated wild-type plants and further enhanced the differentiation of the wild-type plant under red light (Fig. 7; Supplemental Fig. S6). In contrast, GA_9 was

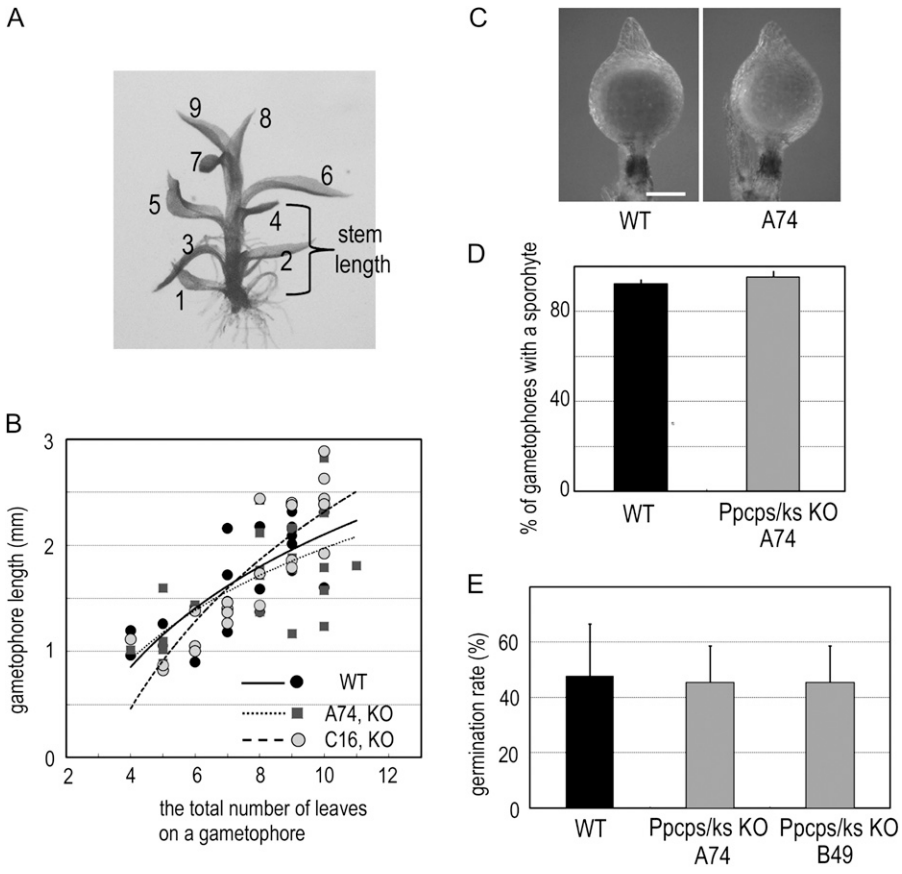

Figure 6. Gametophores, sporophytes, and spore germination rate of *CPS/KS* disruption mutant lines were not distinguishable from those of the wild type. A, A gametophore of the Ppcps/ks KO A74 line. Leaves are numbered from the oldest leaf to the youngest one. B, The relationship between the total number of leaves on a stem and the length of a stem in gametophores of the wild-type and Ppcps/ks KO A74 and C16 lines. The values on each gametophore were measured after cultivation for 3 weeks ($n > 23$). The slopes were calculated by fitting a linear regression line through the data points. C, Sporophytes of wild-type and knockout lines. Bar = 0.3 mm. D, The percentage of gametophores with a sporophyte in the wild type and Ppcps/ks KO A74. Gametophores were cultivated for 12 weeks under gametangia-inductive conditions ($n > 50$). Error bars represent SD. E, Spore germination rate of wild-type and knockout lines. The spores were cultured for 10 d and counted ($n > 300$). Error bars represent SD. WT, Wild type.

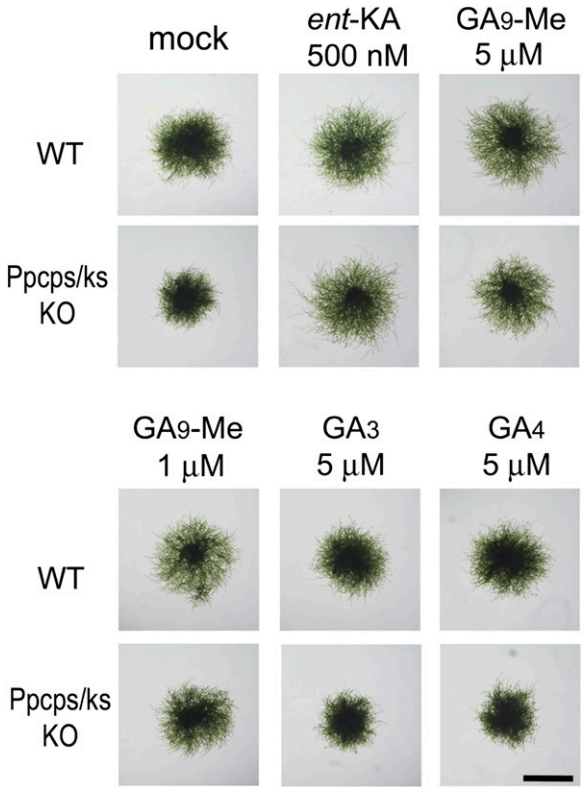

Figure 7. Effects of the GA_3, GA_4, and GA_9 methyl esters on the differentiation to caulonemata in the Ppcps/ks KO mutant. Freshly prepared protonema from wild-type (WT) and knockout plants were cultured on BCD-ATG medium supplemented with *ent*-kaurenoic acid (*ent*-KA), GA_3, GA_4, and GA_9 methyl ester (Me) under red light for 7 d. Representative images of protonemal colonies after cultivation are shown. Bar = 2 mm.

inactive in promoting the differentiation of chloronemata to caulonemata in *P. patens* (Supplemental Fig. S6). Although the GA_9 methyl ester was active in stimulating caulonemal differentiation, its activity was about 10 to 20 times lower than that of *ent*-kaurenoic acid (Supplemental Fig. S6). The GA_{73} methyl ester partially restored the differentiation in the mutant at 10 μM, whereas the GA_3 methyl ester, GA_{103}, and antheridic acid did not (Supplemental Figs. S6 and S7). These results indicate that the bioactive GAs in angiosperms are not the active metabolites that promote caulonematal differentiation in moss. The weak, but significant, activity of the methyl esters of GA_9 and GA_{73} suggests that *P. patens* may have a GA-related metabolite(s) downstream of *ent*-kaurenoic acid that acts as a regulator of protonema development.

Cross Talk of Phytohormones in Caulonema Development

Auxin promotes the differentiation of chloronemata to caulonemata (Imaizumi et al., 2002; Decker et al., 2006). The differentiation was completely inhibited by *α-tert*-butoxycarbonylaminohexyl indole-3-acetic acid (BH-IAA), the specific antagonist of the TIR1/AFB auxin receptors (Hayashi et al., 2008); this inhibition was restored by excess exogenous auxin application. This suggests that SCF^{TIR1} auxin signaling regulates the differentiation of chloronemata to caulonemata. Red light was reported to induce caulonemal formation and to enhance the auxin sensitivity as measured by the early auxin-responsive GH3 promoter activity, which is regulated by the SCF^{TIR1} pathway in *P. patens* (Imaizumi et al., 2002). The light signal transduced by cryptochrome represses the auxin response pathway and reduces the differentiation to caulonemata (Imaizumi et al., 2002). However, the cross talk between auxin and light signaling has not been investigated. We examined whether auxin and light signals are integrated to regulate protonemal development.

BH-IAA inhibited the red light-induced differentiation of chloronemata in wild-type plants; wild-type protonemata treated with BH-IAA phenocopied the protonemata of the Ppcps/ks KO mutant (Fig. 8A). In contrast, caulonemal formation in the Ppcps/ks KO mutant was insensitive to BH-IAA, since the differentiation to caulonemata was already suppressed in the mutant. This suggests that both auxin signaling via the SCF^{TIR1} pathway and *ent*-kaurene signaling are required for red light-promoted differentiation of chloronemata to caulonemata.

To further examine the involvement of *ent*-kaurene metabolites in auxin-regulated protonemal development, the effects of *ent*-kaurene metabolites on auxin-induced caulonemal cell formation in both the wild type and the Ppcps/ks KO mutant were investigated (Fig. 8, B and C). Under white light, the caulonemal cell formation of the mutant was slightly reduced compared with that of the wild type (Fig. 8C). 1-Naphthylacetic acid (NAA) treatment enhanced caulonemal cell formation in both wild-type and mutant plants, but the mutant was less responsive to NAA than the wild type (Fig. 8, B and C). The reduced auxin responsiveness of the mutant was restored to the wild-type level in the presence of *ent*-kaurene or *ent*-kaurenoic acid (Fig. 8, B and C). *ent*-Kaurene or *ent*-kaurenoic acid supplied at 5 μM further enhanced caulonemal cell formation in the wild type (Fig. 8C). 16-Hydroxy *ent*-kaurane is a by-product of PpCPS/KS and would not be converted to *ent*-kaurenoic acid (Von Schwartzenberg et al., 2004; Hayashi et al., 2006). 16-Hydroxy *ent*-kaurane, GA_3, and AMO-1618 did not affect auxin-induced caulonemal cell formation under white light (Fig. 8C); these findings were consistent with the results from experiments performed under red light (Fig. 7; Supplemental Figs. S5 and S6). Overall, these results demonstrate that *ent*-kaurenoic acid or one or several *ent*-kaurenoic acid-derived metabolite(s) is involved in the cross talk between the light and auxin signals.

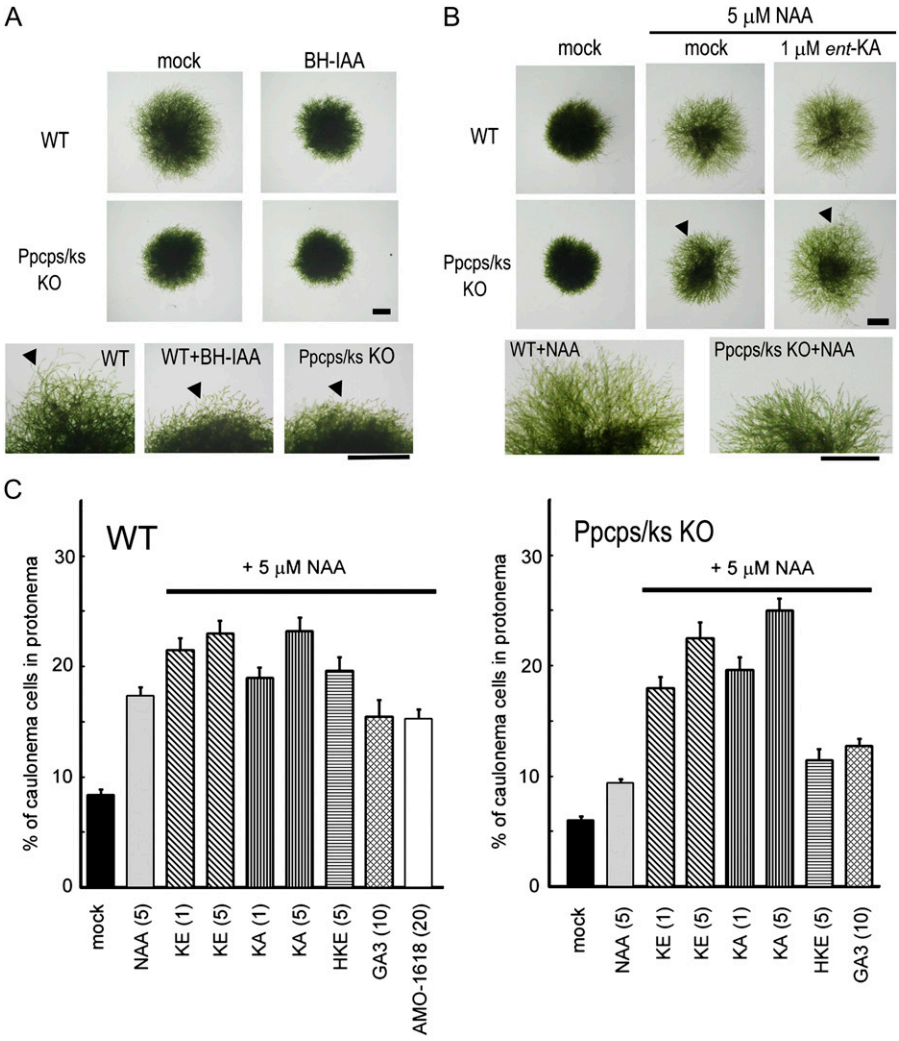

Figure 8. Effects of auxin and *ent*-kaurene-related compounds on the differentiation to caulonemata of *P. patens*. A, Caulonemal protrusions of protonemal colonies treated with BH-IAA, a TIR1 auxin receptor antagonist, were diminished like those of the Ppcps/ks KO deletion mutant. Protonemata were inoculated on BCD-ATG medium with or without 20 μM BH-IAA and cultivated under red light for 8 d. Arrowheads indicate representative caulonemal protrusions. B, The Ppcps/ks KO mutant showed resistance to auxin-induced caulonemal formation. *ent*-Kaurenoic acid (*ent*-KA) restored auxin sensitivity of protonema in Ppcps/ks KO mutants. The protonemal colony was cultured for 8 d under white light in the presence or absence of *ent*-kaurenoic acid with 5 μM NAA. Bars in A and B = 1 mm. C, The effects of *ent*-kaurene-related compounds on auxin-induced caulonemal formation. KE, *ent*-Kaurene; KA, *ent*-kaurenoic acid; HKE, 16-hydroxy *ent*-kaurane. The values in parentheses show the concentrations of chemicals (μM). The ratio of caulonemal cells in protonemata was counted after the cultivation of protonemata under white light for 9 d on BCD-ATG medium containing chemicals and 5 μM NAA. All values are averages of 100 protonemal cells examined. Error bars represents SD. WT, Wild type.

DISCUSSION

Diterpene Metabolites from *ent*-Kaurene Are Involved in Protonemal Differentiation

The loss of *ent*-kaurene production affected the differentiation of protonemal cells in *P. patens*. The differentiation of chloronemata to caulonemata was reduced in Ppcps/ks KO mutant lines. This reduced differentiation was clearly observed during caulonema-inducing growth conditions (auxin treatment and red light irradiation). The reduction in differentiation to caulonemata was restored by the exogenous application of *ent*-kaurene or *ent*-kaurenoic acid. These results demonstrate that diterpene metabolites from *ent*-kaurene via *ent*-kaurenoic acid participate in the regulation of protonemal development (Fig. 9 shows a working model). If *P. patens* synthesizes GA-like diterpenes from *ent*-kaurene, and such diterpenes show similar elongation effects to those observed in angiosperm GA, then PpCPS/KS disruption mutants would be expected to show reduced elongation of protonemata, gamosphores, or sporophytes. However, loss of PpCPS/KS function does not cause any elongation phenotypes (Figs. 4 and 6B). In summary, the diterpene from *ent*-kaurene would not be involved in cell elongation of *P. patens*.

One of the typical GA responses of seed plants is the promotion of seed germination. By analogy, therefore, it is possible that the diterpene metabolites from *ent*-kaurene might enhance spore germination. AMO-1618, an inhibitor of CPS, was reported to not only inhibit the enzyme activity of heterologously expressed PpCPS/KS in *Escherichia coli* but also to repress the spore germination of *P. patens*. Exogenous *ent*-kaurene rescues the inhibition of spore germination by AMO-1618 (Anterola et al., 2009). However, in our assay, the spore germination rate of the Ppcps/ks KO mutant was identical to that of the wild-type plant (Fig. 6E). The nonspecific effects of AMO-1618 inhibitor on the component(s) regulating spore germination could account for these differences.

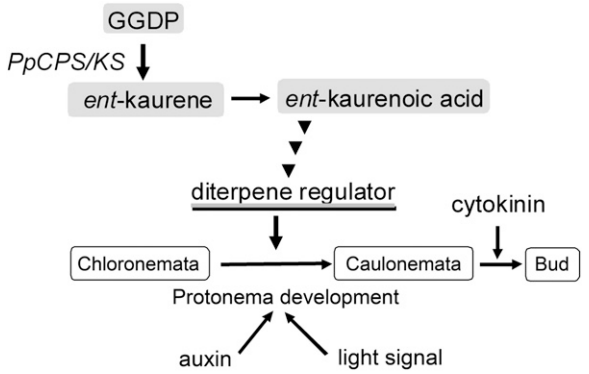

Figure 9. A model of the physiological role of diterpene regulators from *ent*-kaurene. *ent*-Kaurene was synthesized from GGDP and then converted to *ent*-kaurenoic acid. The GA-type diterpenes from *ent*-kaurenoic acid positively regulate the differentiation to caulonemata, in cooperation with auxin and light signals.

Diterpene Metabolites from *ent*-Kaurene Are GA Methyl Ester?

Here, we demonstrate that diterpene metabolites from *ent*-kaurene via *ent*-kaurenoic acid participate in the regulation of protonemal development. These diterpene metabolites would likely be endogenous growth regulators for the differentiation from chloronemata to caulonemata, acting in cooperation with auxin and light signals.

The lycopod *S. moellendorffii* biosynthesizes GA_4 as an endogenous active GA and has a functional GID1-DELLA signaling component(s). In contrast to the potent GA effects on angiosperms, exogenously applied GA_4 (10 μM) did not dramatically promote the stem elongation of *S. moellendorffii*; the application of uniconazole, a GA biosynthesis inhibitor, did not cause the severe dwarf phenotype (Hirano et al., 2007). These findings suggest that the physiological role of GA is of limited significance on lycopod growth, although fundamental GID1-DELLA signaling components(s) would function in the lycopod. *S. moellendorffii* utilizes GA-type diterpenes as an antheridiogen (an antheridium-inducing hormone), such as GA_9 methyl ester, GA_{73} methyl ester, and antheridic acid (Nester et al., 1987; Yamane et al., 1988; Yamauchi et al., 1996, 1997; Yamane, 1998; Kurumatani et al., 2001). These antheridiogens showed potent biological activity for the induction of antheridia at the picomolar to nanomolar range. However, GA_9 methyl ester showed low affinity to SmGID1 in contrast to high affinity of GA_4 (Hirano et al., 2007). These lines of evidence imply that the lycopod might utilize a distinct pathway for the perception of GA_4 and antheridium-inducing GAs.

Our work demonstrates that exogenous treatment with *ent*-kaurene or *ent*-kaurenoic acid complemented the protonemal defects in Ppcps/ks KO mutants within a physiologically relevant nanomolar to micromolar range, while at these concentrations GA_3 and GA_4 did not complement the protonemal defects. The results presented here imply that the moss *P. patens* produces endogenous diterpene growth regulators from *ent*-kaurene; the active diterpene is different from active GA for angiosperms. Surprisingly, the GA_9 methyl ester rescued the protonemal phenotype of the *PpCPS/KS* disruption mutant. Hirano et al. (2007) reported that GA_9 and the GA_9 methyl ester did not promote the interaction of PpGID1 and PpDELLA homologs in a yeast two-hybrid assay. Therefore, the GA_9 methyl ester would not be recognized by the moss GID1-DELLA pathway if the pathway is functional in the moss. The complementary effects of GA_9 methyl ester on the differentiation to caulonema of the mutant were approximately 10 to 20 times less active than those of *ent*-kaurenoic acid. Additionally, no trace of GA_9 was detected in *P. patens* by LC-MS/MS analysis. These findings suggest that the GA_9 methyl ester is not a true endogenous regulator derived from *ent*-kaurenoic acid in *P. patens*, although the possibility that these compounds were below the limits of detection cannot be ruled out. The GA_{73} methyl ester, a dehydrated 9,11-ene derivative of GA_9 methyl ester, partially restored the phenotype of the disruption mutants (Supplemental Fig. S7). However, the GA_{73} methyl ester was considerably less active than the GA_9 methyl ester. Additionally, the GA_3 methyl ester was inactive to the caulonemal formation of mutant. These results suggest that *P. patens* strictly recognizes the structure of the GA-type endogenous regulator for protonemal differentiation.

Cross Talk of *ent*-Kaurene-Derived Metabolites with Auxin and Light in Protonema Differentiation

In seed plants, auxin and GA both regulate cell elongation and tissue differentiation. Auxin affects GA signaling and biosynthesis (Swarup et al., 2002; Weiss and Ori, 2007). In Arabidopsis, root elongation induced by GA requires auxin. Auxin promotes the GA-dependent DELLA protein degradation in root cells, leading to the regulation of GA-induced root elongation (Fu and Harberd, 2003). Auxin also affects GA biosynthesis by positively regulating the expression of GA biosynthetic genes (O'Neill and Ross, 2002; Frigerio et al., 2006; Nemhauser et al., 2006). This auxin effect on GA biosynthesis was shown to be mediated via the degradation of the Aux/IAA repressor of auxin signaling (Frigerio et al., 2006). Auxin, as well as GA, is closely involved with many other light-regulated developmental processes, including hypocotyl elongation, shade avoidance, and photomorphogenesis.

In the moss *P. patens*, the differentiation from chloronemata to caulonemata is regulated by auxin and light signals (Imaizumi et al., 2002). An auxin antagonist (BH-IAA) specific to the TIR1/AFB auxin receptors completely inhibited auxin-induced differentiation to caulonemata. This indicates that the auxin signal via the SCF^{TIR1} pathway could be a major regulatory signal

in the differentiation to caulonemata. The auxin-responsive *GH3* promoter is rapidly induced by the auxin signal via the SCF^{TIR1} pathway, and red light enhances auxin sensitivity of GH3 promoter activity on the differentiation to caulonemata (Imaizumi et al., 2002). In contrast, the blue light signal transduced via cryptochrome represses both the auxin sensitivity of the *GH3* promoter and, therefore, the differentiation to caulonemata (Imaizumi et al., 2002). Thus, auxin and light signals in *P. patens* are integrated to regulate protonemal differentiation. If a diterpene hormone from *ent*-kaurene is present in the moss, it is likely that such a diterpene growth regulator would interact with other hormones and a light signal to regulate this developmental process. In this study, we demonstrated that the disruption of *ent*-kaurene production in *P. patens* not only confers the auxin resistance in protonemal development but also affects the photomorphogenesis of protonemata. The inhibition of SCF^{TIR1} signaling by auxin antagonists blocked red light-induced differentiation to caulonemata, and the wild type treated with auxin antagonists phenocopied the knockout mutant. These results imply that diterpene metabolites from *ent*-kaurene are involved in the auxin and light signals regulating protonemal differentiation.

Our results raised many questions. Are the moss diterpene regulators from *ent*-kaurene structurally related to GAs active in higher plants? Are GA-type regulators universally present among the various moss species? If so, are active GA-type regulators common compounds among the different mosses, as with active GAs in angiosperms, or is there variation, as in the case of the lycopod antheridiogen? How does the moss biosynthesize the active diterpenes from *ent*-kaurenoic acid? Do the moss GID1 and DELLA homologs recognize the active diterpene regulators? Is there a new signaling pathway in the moss for the perception of GA-type diterpene regulators? The answers to these questions will be the subject of further investigation. Our study provides a basis for this future work by offering new insight into the evolution of diterpene hormones of land plants that lead to GA perception and biosynthesis in seed plants.

MATERIALS AND METHODS

Plant Materials, Growth Conditions, and Transformation

The wild-type strain of *Physcomitrella patens* subsp. *patens* (Ashton and Cove, 1977) was used. Protonemata cells of *P. patens* were cultivated aseptically on BCD-ATG medium (Nishiyama et al., 2000) under continuous fluorescent white light at 24°C. A red light-emitting diode light (ISL-150X150-RB; CCS) with an intensity of 14 μmol m^{-2} s^{-1} was used as a light source. Polyethylene glycol-mediated transformation was performed as described previously (Nishiyama et al., 2000).

Chemicals

ent-Kaurene was extracted from the leaf of *Cryptomeria japonica* by reflux with *n*-hexane; the extract was then purified by silica gel column chromatography and eluted with hexane. *ent*-Kaurene was recrystallized from the hexane-ethanol solvent. The compound 16-hydroxy *ent*-kaurane was isolated from *P. patens* protonemata by solvent extraction with acetone and repeated silica gel column chromatography. The GA_9 and GA_3 methyl esters were synthesized by the esterification of the corresponding GAs using diazomethane. AMO-1618 and uniconazole were purchased from Merck Chemicals and Wako Pure Chemical Industries, respectively.

GC-MS and LC-MS Analysis of *ent*-Kaurene-Related Compounds

ent-Kaurene and 16-hydroxy *ent*-kaurane were measured by GC-MS. Exactly 0.1 g of *P. patens* protonemata (fresh weight) was extracted with 2.5 mL of *n*-hexane. The hexane solution (1 μL) was directly injected into the GC-MS instrument (JMS-Bu25 GCMate; JEOL). The GC-MS conditions used were described previously (Hayashi et al., 2006).

To quantify *ent*-kaurenoic acid, frozen tissues were extracted with 80% (v/v) aqueous acetone and homogenized with a blender. For quantitative analysis (Table I), *ent*-[17,17-$^2H_2$]kaurenoic acid was added to the extract as an internal standard, but this step was omitted for the purpose of identification (Supplemental Fig. S2). Extracts were evaporated in vacuo, dissolved in 50% aqueous acetonitrile, and partitioned against an equal volume of *n*-hexane. The 50% acetonitrile fraction was collected, evaporated under vacuum, and resuspended in water. The sample was loaded onto a hydrophilic-lipophilic-balanced reverse-phase cartridge column (Oasis HLB; 50 mg; Waters), washed with 40% aqueous acetonitrile containing 1% acetic acid, and then eluted with 80% aqueous acetonitrile containing 1% acetic acid. The eluate was evaporated to dryness, dissolved in methanol, and loaded onto a diethyl amino cartridge column (Bond Elut; Varian). After washing with methanol, the acidic compounds were eluted with methanol containing 0.1% acetic acid. The eluate was evaporated to dryness under vacuum, trimethylsilylated with *N*-methyl-*N*-trimethylsilyltrifluoroacetamide, and then analyzed by GC-MS (Automass Sun; JEOL) using a DB17 capillary column (J&W Scientific; 0.25 mm i.d. $\times$ 30 m, film thickness of 0.25 mm). After injection, the oven temperature was held at 80°C for 1 min, then increased to 200°C at 30°C min^{-1}, followed by a further increase to 240°C at 5°C min^{-1}.

GA analysis was carried out on a quadrupole/time-of-flight tandem mass spectrometer (Q-Tof Premier; Waters) equipped with an Acquity Ultra Performance LC apparatus (Waters) as described previously (Varbanova et al. 2007). [17,17-$^2H_2$]GAs were used as internal standards.

Construction of the Ppcps/ks Disruption Vector

A 1.9-kb genomic DNA fragment from 5′ to *PpCPS/KS* was amplified by the DNA polymerase KOD dash (Toyobo) using the primers 5′-CAACCTCTACGTTTTCCAGGCACTAGAACT-3′ and 5′-CTTCTGTAGAGGCCTGGACATTAACGCT-3′. A 1.2-kb genomic DNA fragment from 3′ to *CPS/KS* was also amplified using the primers 5′-CCACCGTTCTAGACGATTACTTCGATCA-3′ and 5′-GCTTACATGGCAACGTAGATTGATACGA-3′. Each fragment was cloned into pCRII-TOPO (Invitrogen). The 3′ *CPS/KS* genomic fragment was digested with *Xba*I and *Bam*HI and inserted into pTN182 with a G418-resistant cassette (accession no. AB267706) and into pTN186 with a hygromycin-resistant cassette (accession no. AB542059). The 5′ *CPS/KS* genomic fragment was digested with *Apa*I and *Hin*dIII and cloned into each of the vectors. These plasmids were designated *Ppcps/ks-KO-G418* and *Ppcps/ks-KO-Hyg*, respectively. Polyethylene glycol-mediated transformation was performed as described previously (Nishiyama et al., 2000). The selected plants were incubated for an additional 1 week without antibiotics and transferred again onto the selection medium. The stable transformants were selected by PCR using appropriate primer sets to confirm the integration of selection marker into the targeted gene *PpCPS/KS*. PCR-positive clones were further analyzed by Southern gel-blot hybridization.

DNA Gel-Blot Analysis

Genomic DNA was digested with restriction enzymes, run on agarose gels, and transferred to a nylon membrane (Hiwatashi et al., 2001). Probe labeling, hybridization, and detection were performed using the AlkPhos Direct Labeling and Detection System (GE Healthcare). A PCR fragment amplified using *PpCPS/KS-KO-Hyg* as a template with the primers 5′-CCACCGTTCTAGACGATTACTTCGATCA-3′ and 5′-GCTTACATGGCAACGTAGATTGATACGA-3′ was used as a probe.

Phenotype Analyses of *Ppcps/ks* Disruption Mutants

Protonemata were homogenized and inoculated onto BCD-ATG medium and cultured under white light for 5 d. Most protonemata were composed of chloronemata. A chloronema-rich colony less than 1 mm in diameter was inoculated on a six-well titer plate containing medium and then cultured at 24°C. The septa of chloronemal cells are perpendicular and those of caulonemal cells are oblique. Protonemal filaments growing at the edge of a colony were randomly selected to calculate the ratio of caulonema cells to chloronema cells in a colony. A protonemal cell next to a protonema apical cell was classified as chloronemal or caulonemal based on the angle of the septa. The length and width of the third cell from a protonema apical cell was measured after 5 d culture on BCD-AT medium (Nishiyama et al., 2000) under white light. The number of protonemal cells with side branches was counted in 10 protonemal cells from a protonema apical cell using protonemata grown on BCD-ATG medium under red light for 5 d. The growth rate of protonema in BCD-ATG medium (0.2% gellan gum) was analyzed by taking photographs of protonema cells at 3-min intervals. To observe the sporophytes, protonemata were inoculated using peat pellets (Jiffy-7; Jiffy Products International) in a plastic plant box (Asahi Techno Glass) as described previously (Tanahashi et al., 2005). The protonemata inoculated on the peat pellets were cultured at 25°C under 16-h-light/8-h-dark conditions for 1 month and then transferred to 15°C under 8-h-light/16-h-dark conditions. For the determination of spore germination rates, spores were spread on solidified BCD-AT medium (Nishiyama et al., 2000) containing 10 mM $CaCl_2$ and cultured at 25°C under continuous light. Ten days after sowing, the numbers of germinated and ungerminated spores were counted with a stereomicroscope.

Supplemental Data

The following materials are available in the online version of this article.

Supplemental Figure S1. LC-MS/MS chromatograms of GA_4 and d_2-GA_4 in *P. patens* tissue.

Supplemental Figure S2. Identification of *ent*-kaurenoic acid from *P. patens*.

Supplemental Figure S3. GC-MS chromatogram and MS spectra of *ent*-kaurene and 16-hydroxy *ent*-kaurane from wild-type and Ppcps/ks KO *P. patens* protonemata.

Supplemental Figure S4. Effects of *ent*-kaurenoic acid on the differentiation to caulonemata.

Supplemental Figure S5. Effects of AMO-1618 on *P. patens* protonemata.

Supplemental Figure S6. Effects of *ent*-kaurenoic acid, GA_9 methyl ester, GA_3 methyl ester, GA_3, GA_4, and GA_9 on the differentiation to caulonemata.

Supplemental Figure S7. Effects of GA-related compounds on the differentiation of chloronemata to caulonemata.

ACKNOWLEDGMENTS

We thank Misako Goto, Etsuko Aoki, Michiko Ichikawa, and Rieko Kakigi at ERATO, Japan Science and Technology Agency, for moss transformation and Dr. Stefan Kepinski at the University of Leeds for critical reading of the manuscript.

Received April 21, 2010; accepted May 18, 2010; published May 20, 2010.

LITERATURE CITED

Anterola A, Shanle E, Mansouri K, Schuette S, Renzaglia K (2009) Gibberellin precursor is involved in spore germination in the moss *Physcomitrella patens*. Planta **229:** 1003–1007

Ashton NW, Cove D (1977) The isolation and preliminary characterization of auxotrophic mutants of the moss, *Physcomitrella patens*. Mol Gen Genet **154:** 87–95

Cho SH, von Schwartzenberg K, Quatrano R (2009) The role of abscisic acid in stress tolerance. *In* C Knight, P-F Perroud, D Cove, eds, The Moss *Physcomitrella patens*. Wiley-Blackwell, West Sussex, UK, pp 282–297

Chopra RN, Kumra PK (1988) Biology of Bryophytes. Wiley Essterrn Limited, New Delhi

Chopra RN, Mehta P (1987) Effect of some known growth regulators on growth and fertility in male clones of the moss *Microdus brasiliensis* (Dub.) Ther. J Exp Bot **38:** 331–339

Cove D, Bezanilla M, Harries P, Quatrano R (2006) Mosses as model systems for the study of metabolism and development. Annu Rev Plant Biol **57:** 497–520

Decker EL, Frank W, Sarnighausen E, Reski R (2006) Moss systems biology en route: phytohormones in Physcomitrella development. Plant Biol (Stuttg) **8:** 397–405

Frigerio M, Alabadi D, Perez-Gomez J, Gracia-Cacel L, Phillips AL, Hedden P, Blazquez MA (2006) Transcriptional regulation of gibberellin metabolism genes by auxin signaling in Arabidopsis. Plant Physiol **142:** 553–563

Fu X, Harberd NP (2003) Auxin promotes Arabidopsis root growth by modulating gibberellin response. Nature **421:** 740–743

Hayashi K, Kawaide H, Notomi M, Sakigi Y, Matsuo A, Nozaki H (2006) Identification and functional analysis of bifunctional ent-kaurene synthase from the moss *Physcomitrella patens*. FEBS Lett **580:** 6175–6181

Hayashi K, Tan X, Zheng N, Hatate T, Kimura Y, Kepinski S, Nozaki H (2008) Small-molecule agonists and antagonists of F-box protein-substrate interactions in auxin perception and signaling. Proc Natl Acad Sci USA **105:** 5632–5637

Hirano K, Nakajima M, Asano K, Nishiyama T, Sakakibara H, Kojima M, Katoh E, Xiang H, Tanahashi T, Hasebe M, et al (2007) The GID1-mediated gibberellin perception mechanism is conserved in the lycophyte *Selaginella moellendorffii* but not in the bryophyte *Physcomitrella patens*. Plant Cell **19:** 3058–3079

Hirano K, Ueguchi-Tanaka M, Matsuoka M (2008) GID1-mediated gibberellin signaling in plants. Trends Plant Sci **13:** 192–199

Hiwatashi Y, Nishiyama T, Fujita T, Hasebe M (2001) Establishment of gene-trap and enhancer-trap systems in the moss *Physcomitrella patens*. Plant J **28:** 105–116

Hu J, Mitchum MG, Barnaby N, Ayele BT, Ogawa M, Nam E, Lai WC, Hanada A, Alonso JM, Ecker JR, et al (2008) Potential sites of bioactive gibberellin production during reproductive growth in *Arabidopsis*. Plant Cell **20:** 320–336

Imaizumi T, Kadota A, Hasebe M, Wada M (2002) Cryptochrome light signals control development to suppress auxin sensitivity in the moss *Physcomitrella patens*. Plant Cell **14:** 373–386

Kawaide H (2006) Biochemical and molecular analyses of gibberellin biosynthesis in fungi. Biosci Biotechnol Biochem **70:** 583–590

Kawaide H, Imai R, Sassa T, Kamiya Y (1997) *Ent*-kaurene synthase from the fungus *Phaeosphaeria* sp. L487: cDNA isolation, characterization, and bacterial expression of a bifunctional diterpene cyclase in fungal gibberellin biosynthesis. J Biol Chem **272:** 21706–21712

Khandelwal A, Cho SH, Marella H, Sakata Y, Perround PF, Pan A, Quatrano RS (2010) Role of ABA and ABI3 in desiccation tolerance. Science **327:** 546

Kurumatani M, Yagi K, Murata T, Tezuka M, Mander LN, Nishiyama M, Yama H (2001) Isolation and identification of antheridiogens in the ferns, *Lygodium microphyllum* and *Lygodium reticulatum*. Biosci Biotechnol Biochem **65:** 2311–2314

Nakajima M, Shimada A, Takashi Y, Kim YC, Park SH, Ueguchi-Tanaka M, Suzuki H, Katoh E, Iuchi S, Kobayashi M, et al (2006) Identification and characterization of Arabidopsis gibberellin receptors. Plant J **46:** 880–889

Nemhauser JL, Hong FX, Chory J (2006) Different plant hormones regulate similar processes through largely nonoverlapping transcriptional responses. Cell **126:** 467–475

Nester JE, Veysey F, Coolbaugh RC (1987) Partia1 characterization of an antheridiogen of *Anemia mexicana*: comparison with the antheridiogen of *A. phyllitidis*. Planta **170:** 26–33

Nishiyama T, Hiwatashi Y, Sakakibara I, Kato M, Hasebe M (2000) Tagged mutagenesis and gene-trap in the moss, *Physcomitrella patens* by shuttle mutagenesis. DNA Res **7:** 9–17

Olszewski N, Sun TP, Gubler F (2002) Gibberellin signaling: biosynthesis, catabolism, and response pathways. Plant Cell (Suppl) **14:** S61–S80

O'Neill DP, Ross JJ (2002) Auxin regulation of the gibberellin pathway in Arabidopsis. Plant Physiol **130:** 1974–1982

Phillips AL, Ward DA, Uknes S, Appleford NE, Lange T, Huttly AK, Gaskin P, Graebe JE, Hedden P (1995) Isolation and expression of three gibberellin 20-oxidase cDNA clones from Arabidopsis. Plant Physiol **108:** 1049–1057

Raghavan V (1989) Developmental Biology of Fern Gametophytes. Cambridge University Press, Cambridge, UK

Sakakibara K, Nishiyama T, Sumikawa N, Kofuji R, Murata T, Hasebe M (2003) Involvement of auxin and a homeodomain-leucine zipper I gene in rhizoid development of the moss *Physcomitrella patens*. Development **130:** 4835–4846

Sun TP, Kamiya Y (1994) The *Arabidopsis* GA1 locus encodes the cyclase *ent*-kaurene synthetase A of gibberellin biosynthesis. Plant Cell **6:** 1509–1518

Swain SM, Singh DP, Helliwell CA, Poole AT (2005) Plants with increased expression of ent-kaurene oxidase are resistant to chemical inhibitors of this gibberellin biosynthesis enzyme. Plant Cell Physiol **46:** 284–291

Swarup R, Parry G, Graham N, Allen T, Bennett M (2002) Auxin cross-talk: integration of signalling pathways to control plant development. Plant Mol Biol **49:** 411–426

Tanahashi T, Sumikawa N, Kato M, Hasebe M (2005) Diversification of gene function: homologs of the floral regulator FLO/LFY control the first zygotic cell division in the moss *Physcomitrella patens*. Development **132:** 1727–1736

Toyomasu T, Kawaide H, Ishizaki A, Shinoda S, Otsuka M, Mitsuhashi W, Sassa T (2000) Cloning of a full-length cDNA encoding *ent*-kaurene synthase from *Gibberella fujikuroi*: functional analysis of a bifunctional diterpene cyclase. Biosci Biotechnol Biochem **64:** 660–664

Ueguchi-Tanaka M, Ashikari M, Nakajima M, Itoh H, Katoh E, Kobayashi M, Chow TY, Hsing YI, Kitano H, Yamaguchi I, et al (2005) GIBBERELLIN INSENSITIVE DWARF1 encodes a soluble receptor for gibberellin. Nature **437:** 693–698

Ueguchi-Tanaka M, Nakajima M, Katoh E, Ohmiya H, Asano K, Saji S, Hongyu X, Ashikari M, Kitano H, Yamaguchi I, et al (2007) Molecular interactions of a soluble gibberellin receptor, GID1, with a rice DELLA protein, SLR1, and gibberellin. Plant Cell **19:** 2140–2155

Vandenbussche F, Fierro AC, Wiedemann G, Reski R, Van Der Straeten D (2007) Evolutionary conservation of plant gibberellin signalling pathway components. BMC Plant Biol **7:** 65

Varbanova M, Yamaguchi S, Yang Y, McKelvey K, Hanada A, Borochov R, Yu F, Jikumaru Y, Ross J, Cortes D, et al (2007) Methylation of gibberellins by *Arabidopsis* GAMT1 and GAMT2. Plant Cell **19:** 32–45

Von Maltzahn KE, Macquarrie IG (1958) Effect of gibberellic acid on the growth of protonemata in *Splachnum ampullaceum* (L). Hedw. Nature **181:** 1139–1140

Von Schwartzenberg K, Schultze W, Kassner H (2004) The moss *Physcomitrella patens* releases a tetracyclic diterpene. Plant Cell Rep **22:** 780–786

Weiss D, Ori N (2007) Mechanisms of cross talk between gibberellin and other hormones. Plant Physiol **144:** 1240–1246

Yamaguchi S (2008) Gibberellin metabolism and its regulation. Annu Rev Plant Biol **59:** 225–251

Yamaguchi S, Saito T, Abe H, Yamane H, Murofushi N, Kamiya Y (1996) Molecular cloning and characterization of a cDNA encoding the gibberellin biosynthetic enzyme *ent*-kaurene synthase B from pumpkin (*Cucurbita maxima* L.). Plant J **10:** 203–213

Yamaguchi S, Sun T, Kawaide H, Kamiya Y (1998) The GA2 locus of Arabidopsis thaliana encodes ent-kaurene synthase of gibberellin biosynthesis. Plant Physiol **116:** 1271–1278

Yamane H (1998) Fern antheridiogens. Int Rev Cytol **184:** 1–32

Yamane H, Satoh Y, Nohara K, Nakayama M, Murofushi N, Takahashi N, Takeno K, Furuya M, Furber M, Mander LN (1988) The methyl ester of a new gibberellin, GA_{73}: the principal antheridiogen in *Lygodium japonicum*. Tetrahedron Lett **29:** 3959–3962

Yamauchi T, Oyama N, Yamane H, Murofushi N, Schraudolf H, Pour M, Furber M, Mander LN (1996) Identification of antheridiogens in *Lygodium circinnatum* and *Lygodium flexuosum*. Plant Physiol **111:** 741–745

Yamauchi T, Oyama N, Yamane H, Murofushi N, Schraudolf H, Pour M, Seto H, Mander LN (1997) Biosynthesis of GA_{73} methyl ester in *Lygodium* ferns. Plant Physiol **113:** 773–778

Yasumura Y, Crumpton-Taylor M, Fuentes S, Harberd NP (2007) Step-by-step acquisition of the gibberellin-DELLA growth-regulatory mechanism during land-plant evolution. Curr Biol **17:** 1225–1230